

# Liquid Chromatography–Mass Spectrometry and Proton Nuclear Magnetic Resonance Characterization of Trace Level Condensation Products Formed Between Lactose and the Amine-Containing Diuretic Hydrochlorothiazide

PAUL A. HARMON, WINNIE YIN, WILLIAM E. BOWEN, R. J. TYRRELL, ROBERT A. REED

Merck & Company, Inc., P.O. Box 4, WP78-210, West Point, Pennsylvania 19486

Received 1 July 1999; revised 19 December 1999; accepted 1 March 2000

**ABSTRACT:** Trace levels of condensation products between lactose and the amine-containing diuretic hydrochlorothiazide are formed when a mixture of the two solids containing 30% weight water is heated at 60 °C for 2 weeks. The two most abundant condensation products were characterized by liquid chromatography-mass spectrometry (LC-MS) and proton nuclear magnetic resonance (<sup>1</sup>H NMR) spectroscopy. Under these relatively mild conditions of formation, the amine–lactose reaction products are limited to those involving the elimination of only a single molecule of water, rather than the multiple-water eliminations associated with later stages of the Maillard reaction. The spectroscopic data clearly show that the primary condensation products are cyclic N-substituted glycosylamines rather than Schiff base, 1,2-enolic forms, or Amadori rearrangement products of identical mass. In solution, the two most abundant N-substituted glycosylamines are shown to be in a kinetically slow equilibrium with each other, most likely through a mutarotation involving the intermediate formation of the acyclic Schiff base. © 2000 Wiley-Liss, Inc. and the American Pharmaceutical Association *J Pharm Sci* 89: 920–929, 2000

**Keywords:** Maillard reactions; amine–lactose reactions; glycosylamines (formation of)

## 1. INTRODUCTION

The possible reaction of amine groups of drug entities with carbonyl groups of common tablet excipients, such as lactose, starch, and cellulose, is of obvious pharmaceutical interest. Despite this, amine–carbonyl reactions have been examined largely within the context of the Maillard reaction and its occurrence in the food processing industry. The Maillard or browning reaction is characterized by the formation of brown pigments when solutions containing carbonyl compounds as well as amines, amino acids, or proteins are heated for prolonged periods at elevated temperatures. Extensive work has been carried out to understand the reaction pathways leading to the colored re-

action products and has been reviewed.<sup>1–3</sup> The later stage Maillard reactions are complex and variable, depending on reaction conditions, and involve further dehydration and fission of the initial reaction products. There is general agreement that the initial step in the Maillard reaction involves a condensation between the carbonyl group and the free amino group.

The initial stages of the Maillard reaction thus provide a potential mechanism for covalent linkage of drug compound amine groups with lactose. Several previous studies have examined amine–lactose reactions from a pharmaceutical perspective, but have focused primarily on the mechanism of the browning observed rather than a complete structural determination of the amine–lactose reaction product(s) formed. Duvall et al.<sup>4</sup> prepared aqueous solutions of lactose and amphetamine sulfate and observed browning of the solutions stored at 50 °C for 7 days. Browning

Correspondence to: Paul A. Harmon (Telephone: 215-652-4214; Fax: 215-652-2821)

*Journal of Pharmaceutical Sciences*, Vol. 89, 920–929 (2000)  
© 2000 Wiley-Liss, Inc. and the American Pharmaceutical Association



at 60 V, which represented an optimum for production of both molecular ions as well as fragmentation products. Mass spectra were averaged across the width of an eluted peak, and an averaged background spectrum was subtracted.

### 2.2.3. $^1\text{H}$ NMR

The  $^1\text{H}$  NMR spectra were recorded on a Bruker DMX 300 MHz NMR spectrometer in  $\text{DMSO-d}_6$  with 5% 0.1 N HCl added. Proton chemical shifts were referenced to tetramethylsilane. The  $^1\text{H}$  NMR spectra typically required 2000 scans for a total data acquisition time of ~2.5 h.

## 2.3. Chromatographic Conditions

A mobile phase consisting of 98.5% phosphate buffer (20 mM, pH 2.9) and 1.5% acetonitrile was used with an Alltech Platinum EPS C8 column (25 cm  $\times$  4.6 mm, 5  $\mu\text{m}$  particle size) to separate HCTZ and its degradation product DSA from HCTZ–lactose condensation products. The flow rate was 1.5 mL/min, and the detection wavelength was 270 nm unless UV spectral data were being obtained. The column temperature was ambient. The injection volume was varied to optimize fraction collection as described later.

On-line LC-MS data were obtained with a linear gradient mobile phase that ran from 100% aqueous formic acid (0.1%) to 87% formic acid (0.1%) and 13% acetonitrile over 17 min. The column used was a phenomenex Nucleosil 5 C18 (15 cm  $\times$  4.6 mm, 5  $\mu\text{m}$  particle size). The flow rate was 1.0 mL/min, and the detection wavelength of 270 nm was used unless UV spectral data were being obtained.

## 2.4. HCTZ–Lactose Stressing and Solubilization Procedures

About 2 g of bulk HCTZ, 2 g of bulk lactose, and 2 g of unbuffered HPLC grade water (ambient pH 5.2) were mixed in an amber glass bottle to form a thick, uniform paste. The bottle was then tightly capped and placed in an oven at 60 °C for 2 weeks. Upon removal, no browning of the HCTZ–lactose mixtures was apparent. The stressed HCTZ–lactose mixtures were then worked up in two different ways. The first way was to simply dissolve a portion of the wet solids in a large enough volume of 50% methanol and 50% phosphate buffer (20 mM, pH 2.9) so that all

solids were dissolved. The solution was then diluted a further 10-fold with pH 2.9 phosphate buffer.

The second work up procedure takes advantage of the high water solubility of lactose and the low water solubility of HCTZ, and greatly enhances the quantities of HCTZ–lactose condensation products solubilized compared with unreacted HCTZ. About 2 g of the stressed solids were placed in a flask into which 5 mL of water was added. The resulting slurry was shaken and sonicated intermittently for ~10 min. Several milliliters of a clear solution free of solids could be obtained by filtration through 0.45- $\mu\text{m}$  disposable filters. These “selectively solubilized” solutions were examined by HPLC as well as by on-line LC-MS.

Control experiments were also performed in which no water was added to the HCTZ and lactose mixed solids prior to heating at 60 °C for 2 weeks. The control samples were then treated similarly to the water-added samples. No measurable condensation products were observed.

## 2.5. Sample Preparation for $^1\text{H}$ NMR Experiments

The selectively solubilized aqueous solutions were injected on analytical columns using the HPLC Alltech Platinum EPS C8 column-based method. Using 90- $\mu\text{L}$  injections, fractions of the major HCTZ–lactose condensation product were collected by hand between 5.2 and 5.7 min. Assuming a UV response factor of one compared with HCTZ, fractions corresponding to ~0.5 mg of the primary condensation product were collected. The collected fractions (~15 mL) were concentrated and desalted using an OASIS HLB extraction cartridge. The fractions were loaded, washed with 3 mL of water, and then eluted with 3 mL of methanol. The methanol was then evaporated to dryness with compressed air. The HCTZ–lactose condensation product was then redissolved into 1 g of  $\text{DMSO-d}_6$  and 50  $\mu\text{L}$  of 0.1 N HCl.

# 3. RESULTS AND DISCUSSION

## 3.1. HPLC Analysis

The chromatogram of a 10- $\mu\text{L}$  injection of the HCTZ–lactose stressed slurry after selective solubilization in water is shown in Figure 2. HCTZ elutes at ~6.3 min, whereas the HCTZ hydrolysis degradate DSA (4-amino-6-chloro-1,3-benzene disulfonamide, Figure 1) eluted near 4.3 min and

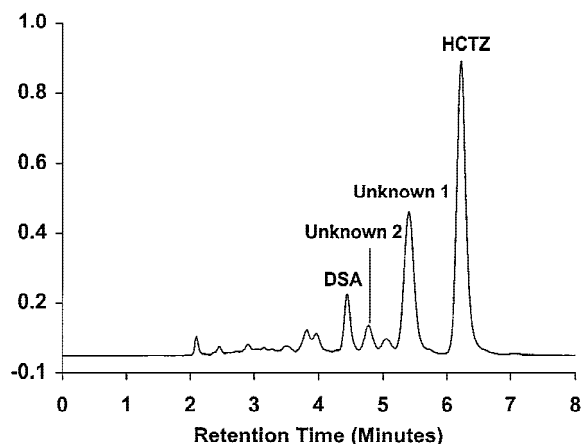


**Figure 2.** Chromatogram of selectively solubilized HCTZ/lactose/water slurry stressed at 60 °C for 2 weeks. The HCTZ, DSA degradate, and unknowns 1 and 2 peaks are indicated.

was identified by a retention time match to authentic DSA. Two major unknowns eluted before HCTZ (indicated as unknown 1 and unknown 2 in Figure 2). These species are more polar than HCTZ but show UV absorption very similar to HCTZ, with maxima near 220, 270, and 320 nm. The abundance of unknowns 1 and 2 relative to HCTZ, as shown in Figure 2, was dramatically increased by the solubilization procedure used. Chromatograms of a solution prepared from the solubilization procedure described, which dissolved all solids, showed that the more abundant unknown 1 was actually formed at only ~0.1% levels compared with unreacted HCTZ.

### 3.2. LC-MS Investigations

The solution injected in Figure 2 was examined by on-line LC-MS. The MS-compatible gradient method gave a similar separation. The unknowns 1 and 2 from Figure 2 were readily correlated to the on-line LC-MS chromatograms by relative peak areas and by injecting fractions of unknowns 1 and 2 chromatographed as in Figure 2. Figures 3–5 show positive ion mode (upper) and negative ion mode (lower) mass spectra of unknown 1, unknown 2, and HCTZ, respectively. Figure 3 shows the unknown 1 molecular ion  $(M+H)^+$  at  $m/z = 622$  in positive ion mode and  $(M-H)^-$  at  $m/z = 620$  in negative ion mode, with chlorine isotope splitting apparent. The molecular weight of 621 amu is consistent with a HCTZ–lactose condensation product formed by the elimination of a single

molecule of water from the parent compounds. The positive and negative ion mode molecular ions shown in Figure 4 for unknown 2 indicate another HCTZ–lactose condensation product of 621 amu. It is also interesting to note that the unresolved species giving the doublet feature near 3.9 min in Figure 2 (eluting just before DSA) both have masses of 609 amu. This result corresponds to that expected from a DSA–lactose initial condensation product.

Indications of which of the three possible HCTZ amine nitrogen atoms (Figure 1) are involved in the covalent linkage to lactose can be derived from the literature, which suggests that primary amino groups undergo condensation more readily than secondary amino groups.<sup>2, 6</sup> The LC-MS data support the notion that the linkage is through the primary sulfonamide nitrogen. The most convincing observation is of the frag-

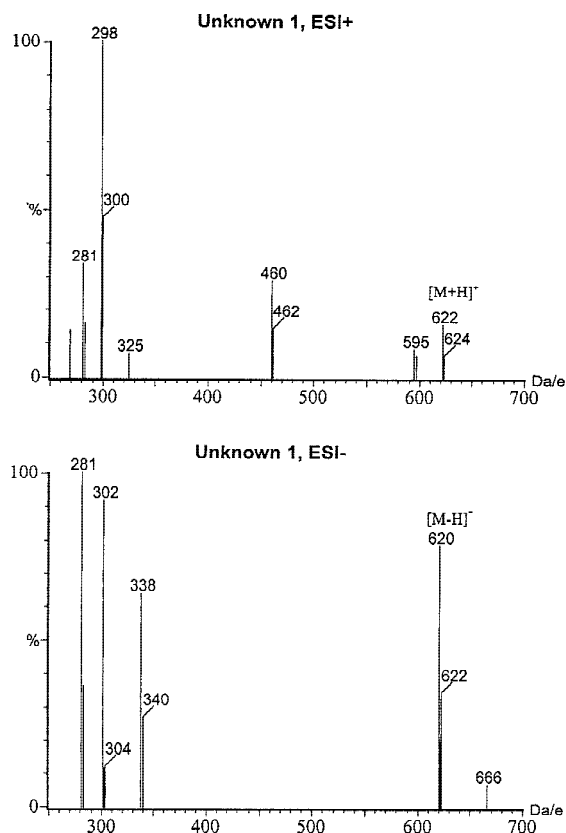


**Figure 3.** Positive ion mode electrospray mass spectrum (upper) and negative ion mode electrospray mass spectrum (lower) of unknown 1. Positive ion mode molecular ion is at  $m/z = 622$  with fragments of  $m/z = 460, 298,$  and  $281$ . Negative ion mode molecular ion is at  $m/z = 620$  with fragments of  $m/z = 338, 302,$  and  $281$ .



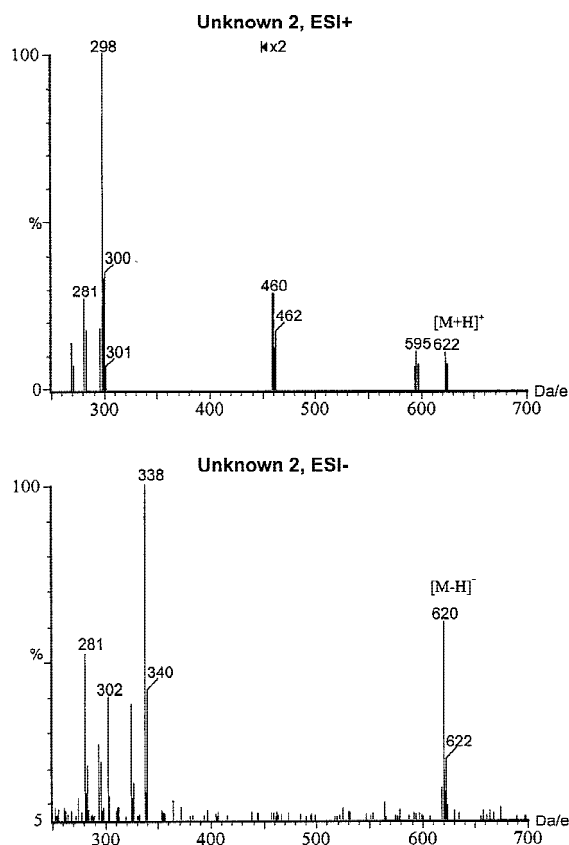


**Figure 4.** Positive ion mode electrospray mass spectrum (upper) and negative ion mode electrospray mass spectrum (lower) of unknown **2**. Positive ion mode molecular ion is at  $m/z = 622$  with fragments of  $m/z = 460$ ,  $298$ , and  $281$ . Negative ion mode molecular ion is at  $m/z = 620$  with fragments of  $m/z = 338$ ,  $302$ , and  $281$ .

ment ions at  $m/z = 338$  and  $302$  in negative ion mode, which are unique to the condensation products. The  $m/z = 302$  fragments do not contain chlorine. Our interpretation of these negative ion fragments is that the  $m/z = 302$  fragment ion is related to some of the same bond-breaking events that gives rise to the  $m/z = 338$  ion, but in which HCl is further eliminated. The elimination of HCl clearly indicates rearrangements occurring near the HCTZ chlorine atom, suggesting the primary sulfonamide nitrogen as the point of covalent attachment to lactose.

General early-stage Maillard reaction pathways have been proposed previously<sup>1,3</sup> and suggest that even at the stage of single water molecule elimination there are five possible structures that might coexist. Assuming the covalent linkage does occur through the primary sulfonamide, the five potential forms are depicted in

Figure 6 for the HCTZ–lactose case. The addition compound could be viewed as formed by nucleophilic attack of the amine on the aldehyde group of the open-ring form of lactose, and is expected to dehydrate readily to give either the acyclic Schiff base (**I**) or cyclic N-substituted glycosylamines (**II**). Weakly acidic conditions can promote an Amadori rearrangement leading to the enolic form (**III**) and the keto tautomer 1-amino-1-deoxy-2-ketose (**IV**). The ketose (**IV**) would be expected to be in equilibrium with the analogous closed-ring structures (**V**). Structures **I–V** of Figure 6 all have molecular weights of 621 amu.

The LC-MS data do not definitively distinguish these five possibilities. For example, the large  $m/z = 298$  positive ions observed in the condensation product mass spectra correspond to the HCTZ molecular ion. Facile formation of HCTZ from the condensation product would seem to ar-

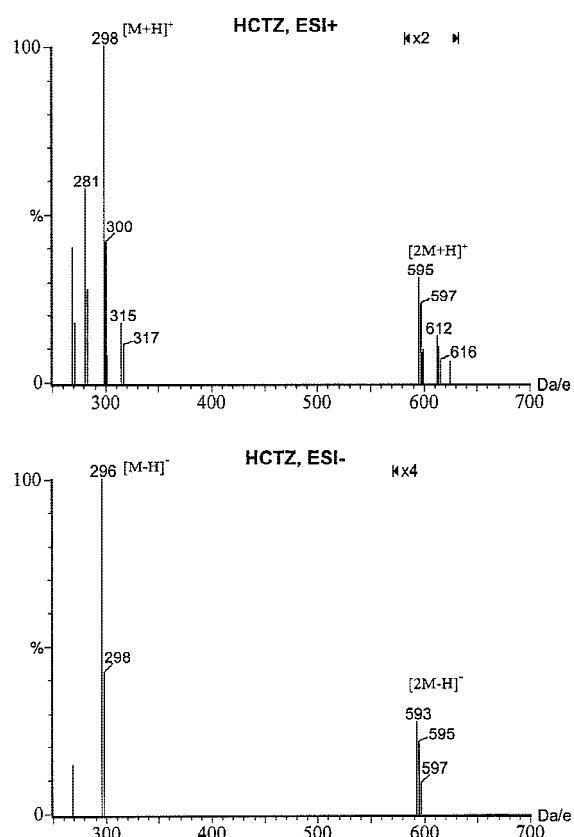


**Figure 5.** Positive ion mode electrospray mass spectrum (upper) and negative ion mode electrospray mass spectrum (lower) of HCTZ. Positive ion mode molecular ion is at  $m/z = 298$  with a major fragment of  $m/z = 281$ . The  $m/z = 595$  peak is due to HCTZ dimer formation. Negative ion mode molecular ion is at  $m/z = 296$ . The  $m/z = 593$  peak is due to dimer formation.

gue against the Schiff base linkage (I) in Figure 6. The  $m/z = 338$  negative ion fragment already discussed would require that two carbon atoms and an oxygen atom from the glucose ring of lactose remain attached to the HCTZ moiety. This type of rearrangement would seem to favor the open-ring structures (II–IV) in Figure 6 because only one single bond would have to be broken.

### 3.3. $^1\text{H}$ NMR Analysis of Major Condensation Product

To discern structures I–V,  $^1\text{H}$  NMR spectra were obtained on the primary HCTZ–lactose condensation product (unknown 1 in Figure 2). Unknown 1 was fractionated using the chromatography in Figure 2, concentrated, and then exchanged into deuterated dimethyl sulfoxide. Figure 7 shows the 7 to 9 ppm region of the  $^1\text{H}$  NMR spectra of HCTZ (top) and of the major HCTZ–lactose condensation product (bottom). The HCTZ assignments in this solvent system have been determined<sup>7</sup> and are indicated on the HCTZ structure in the top of Figure 7. In HCTZ, the peaks arising from the aromatic protons (2 and 6) are sharp and each integrate for one proton. The two hydrogen

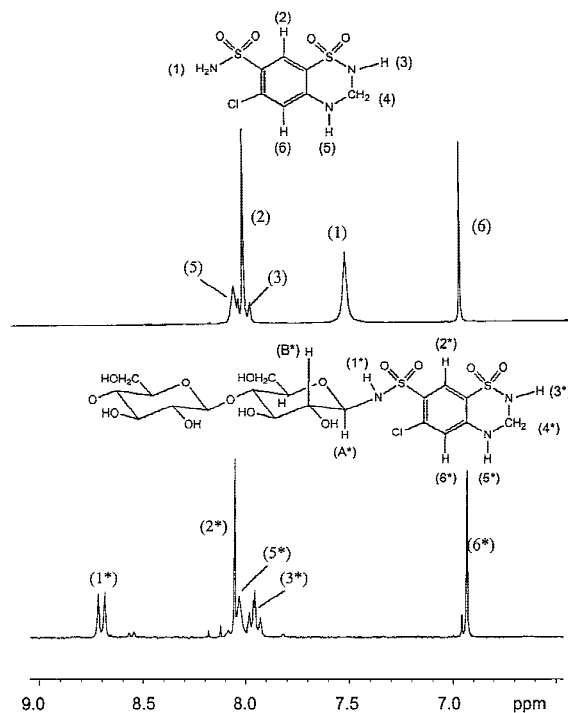


**Figure 7.**  $^1\text{H}$  NMR spectra of HCTZ (top) and the major HCTZ–lactose condensation product (bottom) in the 6–9 ppm region. Assignments are as indicated on the appropriate structures.

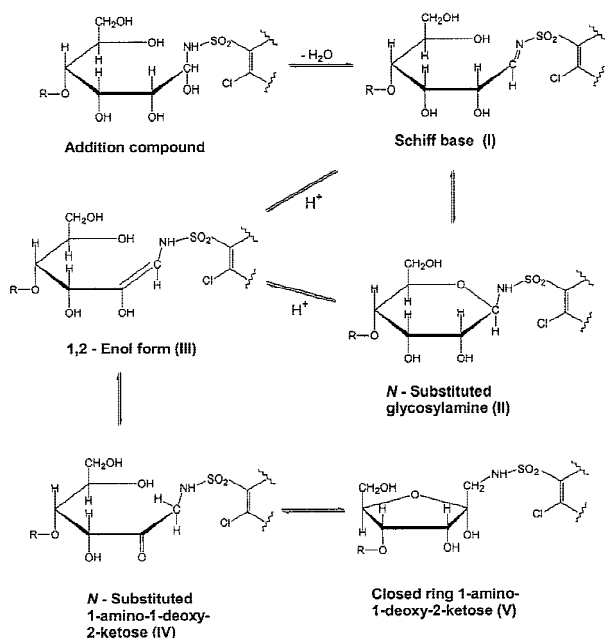


**Figure 6.** Scheme of early stage Maillard reactions adapted from Hodge<sup>3</sup> as applied to HCTZ–lactose condensation through the HCTZ sulfonamide nitrogen. Upon dehydration of the initial addition compound, structures I–V have identical masses.

atoms of the primary sulfonamide (1) give a broader peak near 7.5 ppm that integrates for two protons. The amine proton (5) gives a broad peak near 8.0 ppm, whereas the secondary sulfonamide hydrogen (3) gives a triplet feature, the center peak of which is overlapped with the aromatic proton (2). The entire unresolved multiplet (5, 2, and 3) integrates for the expected three protons. In the condensation product  $^1\text{H}$  NMR spectrum in the bottom portion of Figure 7, the resonances analogous to the HCTZ 5, 2, and 3 protons are obvious and designated 5\*, 2\*, 3\*, respectively, and again integrate for three protons. The fact that the 3\* and 5\* amine protons are observed in the condensation product demonstrates that these nitrogen atoms are not involved in the new covalent bond.

The obvious difference between the two spectra is the downfield shift of the 7.5 ppm HCTZ resonance assigned to the two primary sulfonamide protons (1) to a doublet at 8.7 ppm in the condensation product (coupling constant of 9.9 Hz, designated 1\* in Figure 7) integrating for only a single proton. This result clearly shows that the new covalent bond to lactose is through the pri-

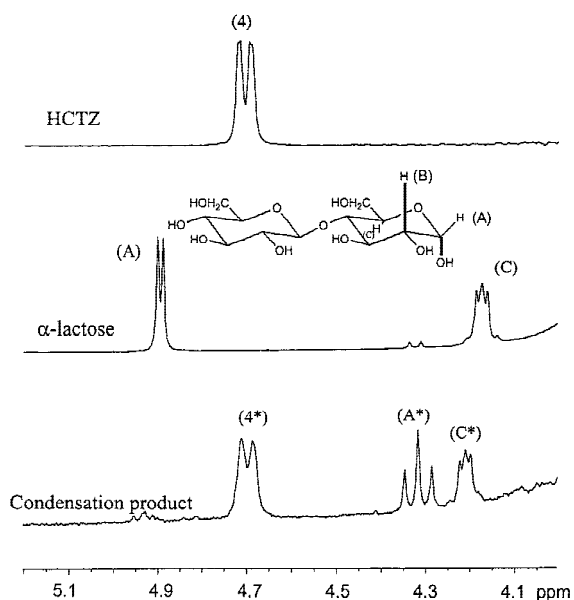


**Figure 8.**  $^1\text{H}$  NMR spectra of HCTZ (top),  $\alpha$ -lactose (middle), and the major condensation product (bottom) in the 6–9 ppm region. Assignments are as indicated on the lactose structure or on the HCTZ and condensation product structures shown in Figure 7.

mary sulfonamide nitrogen. The existence of the 8.7 ppm doublet also excludes the Schiff base type linkage (I) in Figure 6, in which the primary sulfonamide nitrogen would have no protons. This conclusion is consistent with the fact that UV features associated with lactose–amine Schiff base compounds<sup>4,5</sup> are not observed in the UV spectra of the condensation products studied here. Further, the Amadori rearrangement products (IV) and (V) in Figure 6 are ruled out because the sulfonamide proton would be a triplet, rather than the observed doublet. The observed 8.7 ppm doublet is consistent with either the N-substituted glycosylamine (II) or the 1,2-enolic form (III).

Figure 8 shows the 4 to 5 ppm region of the  $^1\text{H}$  NMR spectra of HCTZ (top),  $\alpha$ -lactose (middle), and the condensation product (bottom). The doublet near 4.7 ppm in the HCTZ spectrum is readily assigned<sup>7</sup> to the methylene protons (4) as designated on the HCTZ structure in Figure 7. The  $\alpha$ -lactose spectrum has a doublet near 4.9 ppm (A) due to the proton on the anomeric carbon,<sup>8</sup> and a multiplet due to proton (C) as labeled on the  $\alpha$ -lactose structure in Figure 8. The  $^1\text{H}$  NMR spectrum in the bottom portion of Figure 8 clearly shows the 4\* and C\* protons analogous to the HCTZ (4) protons and lactose (C) protons, respectively. However, in the condensation product,

the lactose doublet from the anomeric carbon proton (A) has shifted upfield from 4.9 to 4.3 ppm, and appears as the triplet (A\*; coupling constant of 9.9 Hz) integrating for one proton. This result is not consistent with the 1,2-enolic condensation product (III) in which the new resonance from the olefinic proton would be expected further downfield as a doublet. The previous exclusion of the Amadori forms (IV and V) is confirmed because the disappearance of the lactose anomeric carbon resonance should be accompanied by the appearance of a new doublet integrating for two protons, rather than the observed 4.3 ppm single proton triplet.

The  $^1\text{H}$  NMR data can only be explained by cyclic N-substituted glycosylamine type structure (II) shown in Figures 6 and 7. The anomeric carbon proton (A\*) appears as a triplet due to similar magnitudes of coupling to both the B\* proton on the lactose ring and the 1\* sulfonamide proton on the HCTZ moiety. This conclusion is readily proven by the decoupling experiment shown in Figure 9. The top  $^1\text{H}$  NMR spectrum of the primary condensation product is redisplayed from Figure 8, whereas the lower spectrum derives from irradiating the 8.7 ppm sulfonamide proton (1\*). The A\* triplet collapses to a doublet with a coupling of 9.0 Hz, revealing the coupling to the B\* lactose proton and confirming the cyclic N-substituted glycosylamine structure (II).

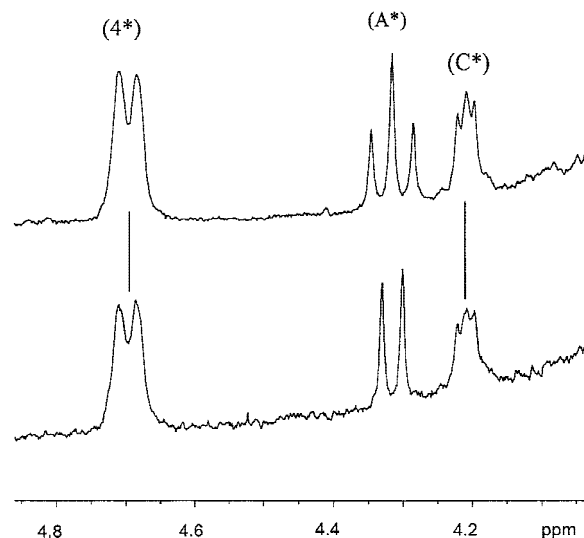


**Figure 9.** Upper: 4 to 5 ppm region of the  $^1\text{H}$  NMR spectrum of the major HCTZ–lactose condensation product redisplayed from Figure 8. Lower: same spectrum when sample is irradiated at the 8.7 ppm sulfonamide proton (1\*, Figure 7). Note the triplet (A\*) collapses to a doublet.

One further aspect of the HCTZ–lactose cyclic N-substituted glycosylamine structure that can be derived from the  $^1\text{H}$  NMR data is the stereochemistry of the anomeric carbon of the lactose. If the HCTZ moiety assumes an equatorial position, then the major condensation product would be designated as the *R*-glycosylamine, whereas if the HCTZ was axial, it would be the *S*-glycosylamine. In  $\alpha$ -lactose, the A proton at 4.9 ppm (Figure 8) due to the proton on the anomeric carbon is equatorial. In  $\beta$ -lactose, the same proton is axial and occurs at 4.3 ppm and can be seen at low levels in the  $\alpha$ -lactose  $^1\text{H}$  NMR spectrum. The 0.6 ppm upfield shift is typical of axial protons that are less deshielded than equatorial protons in 6-membered ring systems. The fact that the A\* proton due to the lactose anomeric carbon proton in the glycosylamine occurs at 4.3 ppm suggests that it is an axial proton and, therefore, that the HCTZ moiety is equatorial and that the glycosylamine is of the *R* configuration. However, this conclusion assumes that the substitution of the hydroxyl group on the anomeric carbon in lactose by the sulfonamide nitrogen moiety of HCTZ in the glycosylamine does not dramatically change the chemical shift of the A\* proton.

More convincing evidence that the A\* proton is axial is the magnitude of the coupling of the A\* proton with the adjacent B\* proton on the lactose ring. For pyran- or cyclohexane-type rings, axial–axial couplings are generally 8–10 Hz, whereas axial–equatorial and equatorial–equatorial couplings are typically 2–3 Hz. This result is borne out for  $\alpha$ -lactose (Figure 8), where the B proton is axial and the A proton is equatorial, and the observed coupling of the A)proton in Figure 8 is 3.5 Hz. The axial–axial coupling between the B and A protons in  $\beta$ -lactose is  $\sim$ 8 Hz from Figure 8. The 9.0 Hz coupling between the A\* and B\*) protons in the glycosylamine revealed by the decoupling experiment confirms that the A\* proton on the anomeric carbon of lactose is axial and that the HCTZ moiety is therefore equatorial position. The major condensation product (unknown 1, Figure 2) is therefore the cyclic N-substituted *R*-glycosylamine.

### 3.4. Mutarotation and Hydrolysis

We noted during isolation procedures that unknown 2 could form slowly from initially pure solutions of the major condensation product. This result is demonstrated in Figure 10. Several fractions of the major condensation product were col-

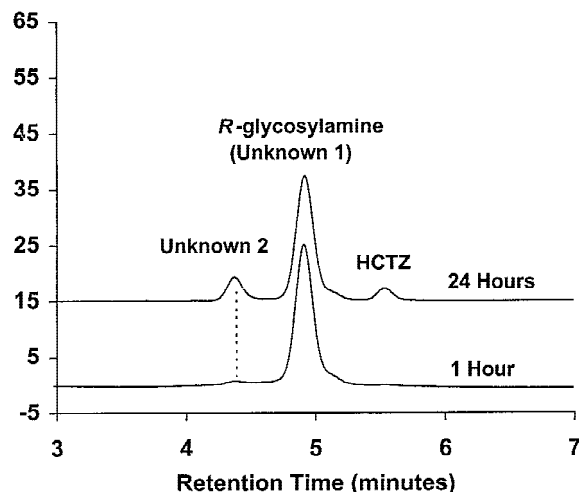


**Figure 10.** Chromatograms of fractions of the *R*-glycosylamine after sitting 1 h (lower) and 24 h (upper) at room temperature, Unknown 2 and some HCTZ forms from the initially pure *R*-glycosylamine.

lected from chromatograms, as in Figure 2, and allowed to sit in the pH 2.9 mobile phase for  $\sim$ 1 h. The sample was then injected, and a typical chromatogram of the resulting sample is shown in the lower portion of Figure 10. After 24 h, the sample was reinjected, and the result is shown as the upper chromatogram in Figure 10. After 24 h,  $\sim$ 15% of the initially pure, cyclic N-substituted *R*-glycosylamine converted to unknown 2. Hydrolysis also occurs to some extent as indicated by formation of HCTZ. The ratio of peak areas of unknown 2 to the major *R*-glycosylamine remains constant thereafter, at about the ratio shown in the upper chromatogram in Figure 10. Similarly, if fractions of unknown 2 are collected, unknown 2 will convert mostly to the *R*-glycosylamine, achieving the same peak area ratio evident in Figure 10.

The behavior shown in Figure 10 is consistent with the known mutarotation of glycosylamines, which has generally been attributed to an equilibrium involving partial conversion of one anomer into the other through intermediate production of the acyclic Schiff base.<sup>6</sup> Varying degrees of hydrolysis may be expected to accompany the mutarotation. If the changes observed in Figure 10 reflect mutarotation, then unknown 2 is the cyclic N-substituted *S*-glycosylamine. This hypothesis is borne out by a closer examination of the  $^1\text{H}$  NMR data in Figures 7 and 8. We realized that 5–10% levels of unknown 2 formed during the isolation and concentration of the *R*-glycosylamine



sample used to generate the  $^1\text{H}$  NMR data. Careful examination of the  $^1\text{H}$  NMR spectrum in the lower portion of Figure 7 reveals a weak doublet near 8.55 ppm, integrating for  $\sim 10\%$  of the nearby  $1^*$  sulfonamide proton doublet of the *R*-glycosylamine. This doublet is consistent with the *S*-glycosylamine sulfonamide proton and has a smaller coupling to the adjacent lactose proton, as expected. Similarly, careful examination of the lower spectrum in Figure 8 shows what appears to be a weak triplet near 4.95 ppm integrating for  $\sim 10\%$  of the  $A^*$  triplet of the *R*-glycosylamine. This result is again consistent with the *S*-glycosylamine, where the equatorial  $A^*$  proton would be expected downfield compared with the *R*-glycosylamine. The identification of unknown **2** as the *S*-glycosylamine condensation product of HCTZ and lactose also explains the nearly identical fragment ions formed in the LC-MS experiments, as shown in Figures 3 and 4.

The relative abundance of the *N*-substituted *R*- and *S*-glycosylamines in the chromatogram in Figure 2 reflects the equilibrium evident in Figure 10. The approximate five-to-one preference shown for the *R* configuration likely derives from the equatorial position of the large HCTZ moiety, which would minimize ring strain compared with the axial position in the *S* configuration. Figure 11 schematically reviews the structures of the HCTZ–lactose *N*-substituted *R*- and *S*-glycosylamine condensation products and their mutarotation in solution. To our knowledge, this is the first report providing detailed structural information of a drug entity amine–lactose condensation reaction product formed under relatively mild reaction conditions.

### 3.5. Pharmaceutical Aspects

Amine–carbonyl condensation reactions typically require elevated temperatures and the presence of water.<sup>6</sup> It is interesting to consider briefly the parameters likely to influence whether or not amine–lactose condensation reactions can occur in formulated tablets upon exposure to the elevated temperatures and humidities typical of accelerated stability conditions. Primary amine groups will be more reactive than secondary or tertiary amines, and the reactivity of the primary amine will increase with increasing basicity.<sup>2,3,6</sup> These trends are demonstrated in this study, where the major condensation products for HCTZ and lactose involved bond formation through the HCTZ primary sulfonamide group rather than ei-

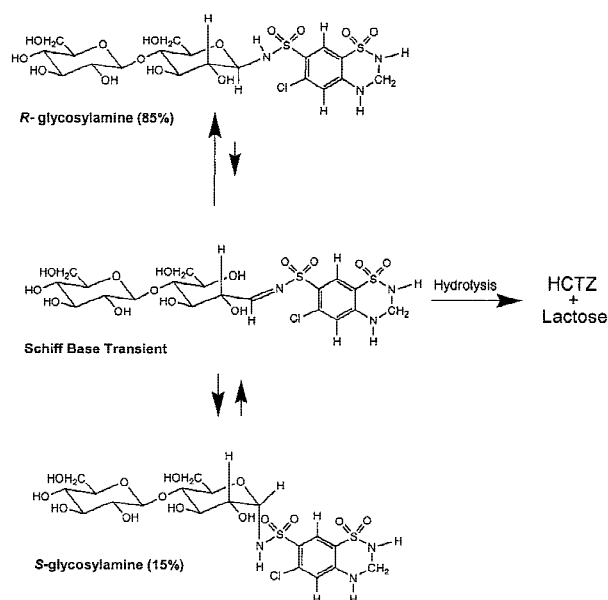


**Figure 11.** Schematic representation of the HCTZ–lactose *N*-substituted *R*- and *S*-glycosylamine condensation products and their mutarotation and hydrolysis in solution.

ther of the secondary amine groups. The role of the basicity of the primary amine is also evident because it explains the large relative abundance of the 609 amu DSA–lactose condensation products eluting near 3.9 min in Figure 2 compared with the total DSA present. The aniline-related primary amine group of DSA (Figure 1) is considerably more basic than the HCTZ primary sulfonamide,<sup>9</sup> leading to condensation of 10–20% of the total DSA present. Given that even aniline is weakly basic on a more general scale of amines, most primary amines would appear basic enough for substantial condensation with lactose under the conditions examined here. In our view, the most critical factor influencing the likelihood of amine–lactose condensation reactions is likely to be the water content of the formulated tablet or the degree to which the tablet is exposed directly to high humidity. Without water, the condensation will not proceed.<sup>2,6</sup> Dry mixtures of HCTZ or DSA and lactose solids formed no measurable HCTZ–lactose or DSA–lactose condensation products when heated at 60 °C. Just how little unbound water is needed to affect these condensations as well as the possible role of bound water from other excipient components will be the subject of a future investigation.

Previous studies have implied that amine–lactose interactions in either tablets or potential

formulations will be reflected by color changes typically associated with later stages of the Maillard reaction.<sup>4,5</sup> Indeed, Castello and Mattocks<sup>10</sup> proposed that a "satisfactory" tablet formulation containing lactose and a primary amine could be determined by preparing a slurry of the ingredients, heating them at 60 °C for a few days, and watching for lack of discoloration. The studies described here serve as a reminder that low levels of initial amine–lactose condensation products may form before any significant browning of excipient solids is observed. Slurries of DSA, lactose, and water prepared and stressed as described for HCTZ and lactose also resulted in no obvious browning. The browning results from further dehydration of the initial amine–lactose condensation products.<sup>1–3</sup> The lack of browning does not prove the initial condensation products are absent.

A final comment regarding the detectability of these types of condensation reaction products is worthwhile. In the present study, lactose is the excipient containing the carbonyl group, and the resulting N-substituted glycosylamine condensation products are relatively low molecular weight species that are water soluble and readily chromatographed. A much more challenging case will be presented to method development chemists if similar condensation reactions can occur between amine groups of drug entities and the carbonyl groups of water-insoluble, polymeric carbohydrates, such as starches and celluloses.

#### 4. CONCLUSIONS

Low levels of HCTZ–lactose condensation products were formed by heating a wet mixture of the two solids at 60 °C for 2 weeks. The structures of the two most abundant condensation products were determined to be the cyclic, N-substituted *R*- and *S*-glycosylamines by LC-MS and <sup>1</sup>H NMR spectroscopy. In solution, the *R* and *S* forms are in

equilibrium with each other through mutarotation, which involves the intermediate formation of the acyclic Schiff base. These studies point out that significant levels of condensation products may be formed without noticeable browning. Formulations of primary amines that contain aldoses should be kept as dry as possible to inhibit possible glycosylamine formation on exposure to elevated temperatures and high humidities.

#### REFERENCES

1. Mauron J. 1981. The Maillard reaction in food; A critical review from the nutritional standpoint. In Eriksson C, editor. *Progress in Food and Nutrition Science*, Vol. 5. New York: Pergamon Press, pp 1–37.
2. Ellis GP. 1959. The Maillard reaction. *Adv Carbohydr Chem* 14:63–134.
3. Hodge JE. 1965. The Amadori rearrangement. *Adv Carbohydr Chem* 10:169–205.
4. Duvall RN, Koshy KT, Pyles JW. 1965. Comparison of reactivity of amphetamine, methamphetamine, and dimethylamphetamine with lactose and related compounds. *J Pharm Sci* 54:607–611.
5. Blaug SM, Huang W. 1972. Interaction of dextroamphetamine sulfate with spray dried lactose. *J Pharm Sci* 61:1770–1775.
6. Ellis GP, Honeyman J. 1955. Glycosylamines. *Adv Carbohydr Chem* 10:95–125.
7. Fang X, Mayr S, Yin W, Harmon PA, Tyrrell RJ, Reed RA. Purification and identification of the dimer impurity in bulk hydrochlorothiazide, manuscript in preparation.
8. Breg J, Romijn D, Van Halbeek H, Vliegthart, JF, Visser RA, Haasnoot CA. 1988. Characterization of four lactose monophosphates by application of <sup>31</sup>P-, <sup>13</sup>C-, and <sup>1</sup>H NMR spectroscopy. *Carbohydr Res* 174:23–36.
9. Deppeler HP. 1981. Hydrochlorothiazide. *Anal Profiles Drug Subs* 10:405–441.
10. Castello RA, Mattocks AM. 1962. Discoloration of tablets containing amines and lactose. *J Pharm Sci* 51:106–108.